Subpixel Unsynchronized Unstructured Light

Chaima El Asmi and Sébastien Roy
Département d'Informatique et de Recherche Opérationnelle, Université de Montréal, Montréal (Québec), Canada

Keywords: Computer Vision, Active Reconstruction, Unstructured Light, Unsynchronized Camera-Projector Systems, Subpixel Accuracy, 3D Scanning.

Abstract: This paper proposes to add subpixel accuracy to the unsynchronized unstructured light method while achieving high-speed dense reconstruction without any camera-projector synchronization. This allows scanning faces which is notoriously difficult due to involuntary movements on the part of the model and the reduced possibilities of 3D scanner approaches such as laser scanners because of speed or eye protection. The unsynchronized unstructured light method achieves this with low-cost hardware and at a high capture and projection frame rate (up to 60 fps). The proposed approach proceeds by complementing a discrete binary coded match with a continuous interpolated code which is matched to subpixel precision. This subpixel matching can even correct for erroneous camera-projector correspondences. The obtained results show that highly accurate unfiltered 3D models can be reconstructed even in difficult capture conditions such as indirect illumination, scene discontinuities, or low hardware quality.

1 INTRODUCTION

The subpixel correspondence is very important in 3D reconstruction as it enables a smooth and dense 3D model. Generally, active reconstruction produces a correspondence where one camera pixel corresponds to one particular projector pixel. On the other hand, by achieving a subpixel correspondence, the accuracy is greatly improved as it improves the matches and enables pixels to be matched to a fractional part of another pixel, as illustrated in Fig. 1.

There are multiple active reconstruction methods that can provide a subpixel correspondence. These methods are divided into two broad categories which can further be split into multiple methods. These methods are referred to as the structured light method and the unstructured light method. The first category consists of projecting several structured light patterns and directly encoding the position of the projector pixel. In this category, the first method is the *Gray Code* (Inokuchi, 1984) and the patterns are composed of white and black stripes at different frequencies. A second method is the *Phase Shift* (Srinivasan et al., 1984) where sinusoidal patterns, composed of the same sine shifted several times at different frequencies, are projected. These methods exhibit many difficulties in scene discontinuities and they are not robust to indirect illumination which in turn leads to multiple matching errors. Several other approaches have tried to improve the *Phase Shift* (Chen et al., 2008; Gupta and Nayar, 2012; Gu et al., 2011). These methods will be detailed in the next section. The second category, unlike the previous one, consists in encoding the position of the projector and the camera in a *LookUp-Table* (LUT) (Kushnir and Kiryati, 2007; Wexler et al., 2003; Couture et al., 2014). The unstructured light method provides bidirectional matching (from camera to projector and from projector to camera). In (Couture et al., 2011), they improved the patterns by generating sines in random directions in the frequency

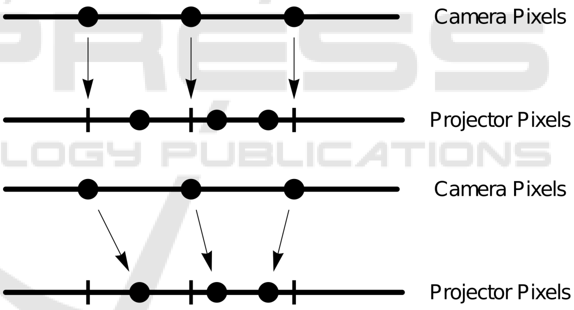

Figure 1: Obtained pixel correspondence between the camera and the projector (top) and a pixel correspondence with subpixel accuracy between the camera and the projector (bottom). This means a pixel can be matched to a fractional part of another pixel. The notches represent the integer position of the corresponding pixels and the dots represent their true position.

El Asmi, C. and Roy, S.
Subpixel Unsynchronized Unstructured Light.
DOI: 10.5220/0007404608650875
In *Proceedings of the 14th International Joint Conference on Computer Vision, Imaging and Computer Graphics Theory and Applications (VISIGRAPP 2019)*, pages 865-875
ISBN: 978-989-758-354-4

domain. Additionally, these patterns don't feature large black and white regions. For this reason, this method is very robust to indirect illumination and scene discontinuities.

The methods presented above must synchronize their projectors and their cameras. Without synchronization, the camera sees mixed projected patterns which results in wrong correspondences. To obtain a correspondence from patterns projected in time, the camera must see each projected pattern by the projector only once. There are two types of synchronization; hardware synchronization (Takei et al., 2007; Zhang et al., 2010; Rusinkiewicz et al., 2002; Liu et al., 2010; Wang et al., 2011) and software synchronization (Herakleous and Poullis, 2014; Koninckx and Van Gool, 2006; Jaeggli et al., 2003). The first type requires expensive and experimental equipment. It consists in synchronizing the projector and the camera using a *triggering circuit* (Liu et al., 2010; Wang et al., 2011). This type of synchronization allows the capture of image sequences at very high frame rate (up to *3000 fps* (Takei et al., 2007)). The second type does not require any experimental material. It is a structured light scan at very low frame rate (usually less than *5 fps*). Unfortunately, this method, with its low frame rate, requires a large amount of time for the camera to fully capture the projected patterns exactly once.

Other methods have performed unsynchronized coded light scans (Sagawa et al., 2014; Moreno et al., 2015; El Asmi and Roy, 2018). The difficulties of the unsynchronized capture reside in finding the first image in the captured sequence and in finding the mixture between two consecutive patterns partially seen by the camera as a single image. Indeed, during the unsynchronized capture at very high frame rate, the camera sees a mixture of two consecutive patterns. It then becomes impossible to get a correspondence between the camera and the projector.

The first method (Moreno et al., 2015) consists in projecting structured light patterns at a high frame rate without synchronization between the projector and the camera. The authors project a looping video of structured light patterns. In order to detect the first image in the captured sequence, they project an easily identifiable sequence of entirely black and entirely white patterns at the beginning of the sequence. They then generate an image formation model of the camera in order to find the synchronization parameters and to recover the patterns corresponding to the *Gray Code*. This method requires complex and very long computations in order to solve the equation systems of the image model. In addition, it is not robust to indirect illumination and scene discontinuities due to the use of *Gray Code*.

Alternative method (El Asmi and Roy, 2018) solved the synchronization problem by projecting a looping video of unstructured light patterns at a high frame rate (*30 to 60 fps*). The camera starts capturing at any time. Thus, it is necessary to find the first image of the captured sequence. They do so by making several correspondences between the captured sequence and the reference sequence which is shifted by one pattern at each correspondence. The first image in the captured sequence is found using the best correspondence after calculating the matching costs. They then find the mixture between the two consecutive patterns by mixing them. The unstructured light patterns are generated randomly so mixing them gives a new random pattern. This method is very fast and simple. It can scan in less than two seconds at *30* or *60 fps*. However, this method does not achieve a correspondence with a high subpixel accuracy. In this paper, we describe a new technique to improve the unsynchronized unstructured light method by matching with a high precision subpixel.

2 PREVIOUS WORK

There are several active methods that achieve a high precision subpixel correspondence. In articles (Salvi et al., 2004; Salvi et al., 2010), a survey on structured light methods is presented. In general, methods that achieve subpixel precision are based on sinusoidal patterns (Wust and Capson, 1991; Zhang and Yau, 2007). The patterns are composed of multiple sines each shifted by a different amount in a given direction and with different frequencies. The sines vary from a very low frequency to a very high frequency. Thus, each camera pixel encodes the projector position directly by a unique phase. This method achieves a dense reconstruction with a high subpixel accuracy through the different gray intensities. However, this method requires photometric calibration because the phase is recovered from the pixel intensities. Furthermore, it is not robust to the indirect illumination which is caused by the low frequency patterns.

In (Chen et al., 2008), they improved the projected patterns by modulating a high frequency signal, so that they are robust to indirect illumination and achieve a high subpixel accuracy. *Modulated Phase Shift* patterns are composed of modulated sines in both directions (two-dimensional patterns) at a very high frequency. Unfortunately, this method requires a very high number of patterns. In (Gu et al., 2011)'s method, they reduced the number of patterns by multiplexing the modulated patterns together. These three methods require what is called the *phase unwrapping* because of the periodic nature of patterns (Huntley and Saldner, 1993; Nayar et al., 2006). Indeed, we must be able to differentiate between the different phases of each period. *Micro Phase Shift* method (Gupta and Nayar, 2012) resolves the problem of *phase unwrapping* by projecting only a high frequency patterns. Alternative methods have used the *Gray Code* (Gühring, 2000) to achieve a subpixel reconstruction. *Line Shifting* (Gühring, 2000) evaluates the subpixel only in the bit transitions (0 to 1 or 1 to 0). However, these alternative methods result in a sparse reconstruction.

In (Martin et al., 2013), they use the unstructured light method to achieve the subpixel accuracy. This method is very robust to indirect illumination and scene discontinuities through their gray level band-pass white noise patterns. They project a lower number of patterns than the method in (Couture et al., 2011). They also improved their technique to generate the codewords (Salvi et al., 2004). By comparing two neighboring codewords, they determine the region where the subpixel is located. They then divide it into four bins by interpolating between the four pixels that define this region. They additionally make a hierarchical vote to choose the right bin and further divide it into another four bins. This operation is repeated recursively several times until they obtain the desired amount of subpixel precision. This method requires a huge calculation time because of the recursion and the hierarchical vote. In this paper, the unsynchronized unstructured light method (El Asmi and Roy, 2018) is improved by accomplishing a high subpixel accuracy. A simple and fast technique to determine the subpixel position is presented in Sec. 4.

3 RELEVANT SUBPIXEL INFORMATION

In establishing pixel correspondence with unstructured light patterns, several parameters have an impact on subpixel accuracy. Amongst these parameters, there is the pattern frequency and the pixel ratio as well as the code-length (linear and quadratic code). Modulating these parameters allow the subpixel accuracy to either improve or degrade.

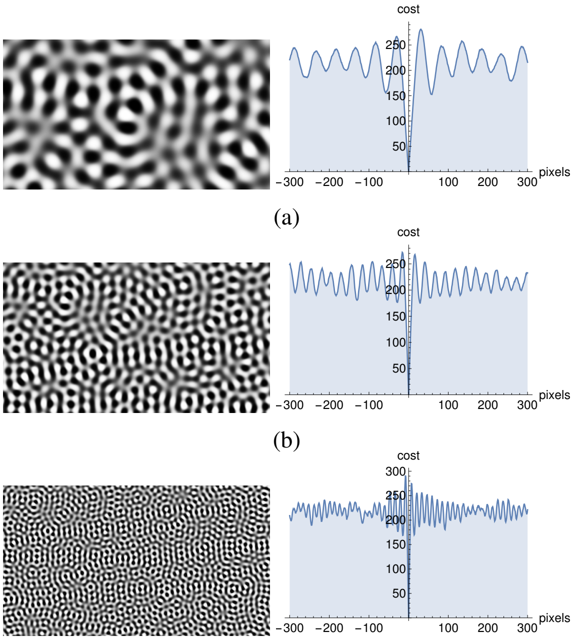

(a)

(b)

(c)

Figure 2: Unstructured light patterns at various spatial frequencies and their cost functions representing the cost of the difference between two neighboring pixels (here, a neighborhood of 300 pixels). The frequency represents the oscillation number of each sine per pattern. Notice that when the frequency increases, the curve is more pronounced. Fig. (a) shows a pattern frequency equal to 25, (b) shows a pattern frequency equal to 50 and (c) shows a pattern frequency equal to 100.

3.1 Pattern Frequency

The unstructured light pattern frequency is the oscillation number of one sine per pattern and is the main property of the unstructured light patterns. Increasing the pattern frequency reduces the impact of indirect illumination and improves matches. Using a very low frequency results in a high correlation between neighboring pixels as they become too similar to match effectively. The subpixel accuracy increases when the frequency is high because the curves of the cost functions are more pronounced and smooth. Fig. 2 shows three patterns with different frequencies and their associated cost function curves. As shown in the figure, the curve becomes more pronounced and precise as the frequency increases. However, using a very high frequency brings about several matching errors because the camera might not be able to distinguish the black and white bands.

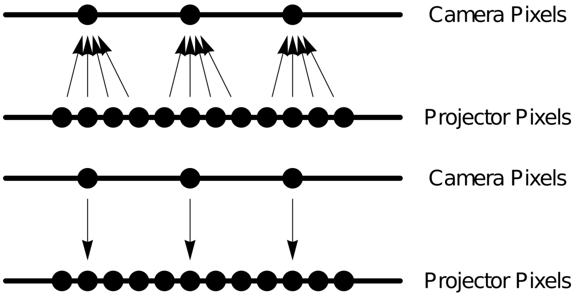

Figure 3: Illustration of pixel ratio where four projector pixels see the same camera pixel (top) and only one camera pixel sees a mixture of four projector pixels (bottom). One can say that the projector-camera correspondences is already subpixel whereas the inverse camera-projector correspondences isn't and it can be improved with a subpixel accuracy.

3.2 Pixel Ratio

The pixel ratio represents the number of pixels seen by a single camera pixel in the projector pattern, and vice versa. The optimal case is for the pixel ratio to be near 1. Indeed, a single pixel of the camera corresponds to only one pixel in the projector. For the current experiments, the pixel ratio is near 2 because the camera sees a mixture of four neighboring pixels in the projector (two pixels per axis). The subpixel accuracy decreases as the pixel ratio increases. To illustrate, consider an example of a pixel ratio near 2. If the camera “sees” four neighboring projector pixels then the correspondence from projector to camera already has a subpixel accuracy of a half pixel per axis. This is because the projector pixels have more information and they are more accurate. As illustrated in Fig. 3, we are already "inside" the camera's pixels. Thus, the pixel ratio is very important in the determination of the subpixel matching, as it can increase or decrease its precision.

3.3 Linear and Quadratic Code

Pixel correspondences between camera and projector are established by using LSH algorithm (Locality Sensitive Hashing) (Andoni and Indyk, 2006). LSH is used in searching for nearest neighbors in very high-dimensional spaces. Because of its inherently random nature, it is necessary to run several LSH iterations. At each iteration, it generates different match proposals and keeps only the best ones based on the difference of bits in the codes. While trying to recover subpixel accuracy, codes from neighboring pixels will be compared. These codes tend to be very similar, so we rely on quadratic code instead of linear code to get enough information.

As described in (El Asmi and Roy, 2018), a linear code with a small number of LSH iterations is used to find the first pattern of the captured sequence and a quadratic code is used to estimate the mixture between two consecutive unstructured light patterns. For a given set of n patterns, a linear codeword is n bits for n bits of information and a quadratic codeword is $\frac{n^2-n}{2}$ bits providing $n\log n$ bits of information, as explained in (Martin et al., 2013). To illustrate, consider an example of 60 patterns, a linear codeword is 60 bits for 60 bits of information and a quadratic codeword is 1770 bits for 354 bits of information. Thus, the quadratic code increases the amount of information and reduces the LSH matching errors. By increasing the number of bits, the quadratic code increases the number of transitions (0 to 1 or 1 to 0) between neighboring pixels by a factor $\log n$ (in our example, $\frac{354}{60} \approx 6$). This increases the subpixel accuracy since it relies on those bit transitions.

4 SUBPIXEL ACCURACY

In order to establish the pixel correspondences between the camera and the projector, an unsynchronized unstructured light method is used (El Asmi and Roy, 2018). Because this method provides bidirectionality of the matches (camera to projector and projector to camera), our method will achieve subpixel accuracy in both directions. For simplicity, only the process of estimating the subpixel correspondences from the projector to the camera will be described. As explained in the previous section, subpixel matching assumes that a projector pixel is observing a mixture of two adjacent pixels in the camera image. This mixture can be described by the parameters (δ_x, δ_y) which represent a non integral displacement from an original integer match $(\hat{x}, \hat{y})$.

4.1 Selecting the Right Quadrant

Before finding the subpixel camera position for any projector pixel, the discrete projector to camera correspondence must be established by using the LSH algorithm. We thus start with a discrete match between projector pixel $\mathbf{p}'$ and camera pixel $\mathbf{p} = (\hat{x}, \hat{y})$ to which a subpixel displacement (δ_x, δ_y) is added to yield the exact match. To estimate the subpixel displacement (δ_x, δ_y), it is necessary to select the quadrant which contains pixel $\mathbf{p}$ and its three neighboring pixels. The subpixel position $(\hat{x} + \delta_x, \hat{y} + \delta_y)$ is located between those four pixels of the camera which are represented by

$$x \leq \hat{x} + \delta_x = x + \lambda_x < x + 1, \quad x = \lfloor \hat{x} + \delta_x \rfloor \tag{1}$$

$$y \leq \hat{y} + \delta_y = y + \lambda_y < y + 1, \quad y = \lfloor \hat{y} + \delta_y \rfloor \tag{2}$$

so we can represent the subpixel position $(\hat{x} + \delta_x, \hat{y} + \delta_y)$ as $(x + \lambda_x, y + \lambda_y)$ where $0 \leq \lambda_x < 1$ and $0 \leq \lambda_y < 1$.

Because the chosen approach uses the unsynchronized unstructured method, it is possible that the projected patterns are mixed temporally in the camera image. This mixture is always computed individually for each camera pixel. For the case of subpixel matching from projector to camera, the four camera pixels forming the quadrant will each feature a different temporal mixture. In the case of camera to projector matching, a single mixture value will be shared by the four projector pixels forming the quadrant. In all cases, the temporal mixture must be applied before a spatial interpolation in order to obtain accurate subpixel matches.

4.2 Estimating the Subpixel Position

The subpixel position (λ_x, λ_y) is located inside the region between the four selected neighboring pixels $\{(x,y),(x+1,y),(x,y+1),(x+1,y+1)\}$. Image intensities will be derived through bilinear interpolation over the quadrant with the parameters (λ_x, λ_y), defined as :

$$\begin{aligned} I[x+\lambda_x, y+\lambda_y] \;=\; & (1-\lambda_y) I[x+\lambda_x, y] \\ & + \lambda_y I[x+\lambda_x, y+1] \end{aligned} \tag{3}$$

where

$$I[x+\lambda_x, y] = (1-\lambda_x) I[x,y] + \lambda_x I[x+1,y] \tag{4}$$

with $0 \leq \lambda_x, \lambda_y < 1$.

In order to obtain the binary code of a pixel, we select a number of intensity pairs from its codeword and subtract them to get intensity differences. These intensities are then binarized to provide the binary code used by LSH for matching.

$$\begin{aligned} & V[x,y] = I_i[x,y] - I_j[x,y] \\ & \qquad\qquad \forall (i,j) \text{ selected intensity pairs} \end{aligned} \tag{5}$$

The intensity difference vector V is then binarized into the code C as

$$C[x,y] = binarize(V[x,y]) \tag{6}$$

where $binarize(x)$ is 1 if $x > 0$, 0 if $x < 0$ and a random sample from $\{0,1\}$ when $x = 0$.

The idea for subpixel matching is that the camera code will best match a projector code which is obtained from image intensities which are interpolated according to the subpixel position. In practice, codes are quantized so they change in steps, which is hard to minimize. By using the non quantized vectors $V[x+\lambda_x, y+\lambda_y]$, the cost can be made continuous and easier to minimize using gradient descent.

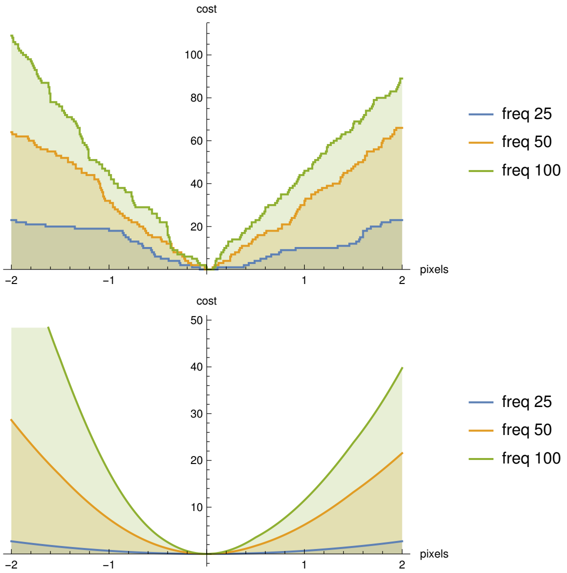

Figure 4: Pattern frequency representing the number of oscillations of one sine in an unstructured light pattern. The blue, orange and green curves correspond to a frequency of 25, 50 and 100 oscillations, respectively. These curves are a cost function of the difference between neighboring pixels. The curves (top) represent a binary difference between the pixel codes and the curves (bottom) represent a continuous difference of two vectors consisting of pixel intensities.

4.3 From Binary Cost Function to Continuous Cost Function

Instead of quantizing the pattern intensity differences V into a binary code C, we directly use V to compute the subpixel value. Two vectors are calculated; the first one, V represents the intensity differences of the pixel $\mathbf{p}$ while the second one, V', which is a reference vector, representing the corresponding coding intensities of the pixel $\mathbf{p}'$.

The subpixel optimization will minimize the angle between vectors V and V', so the objective function is simply defined as

$$\begin{aligned} & cost[x+\lambda_x, y+\lambda_y] = \\ & \qquad angle(V[x+\lambda_x, y+\lambda_y], V'[x,y]) \end{aligned} \tag{7}$$

where

$$angle(a,b) = \arccos\left(\frac{a \cdot b}{\|a\|\|b\|}\right) \tag{8}$$

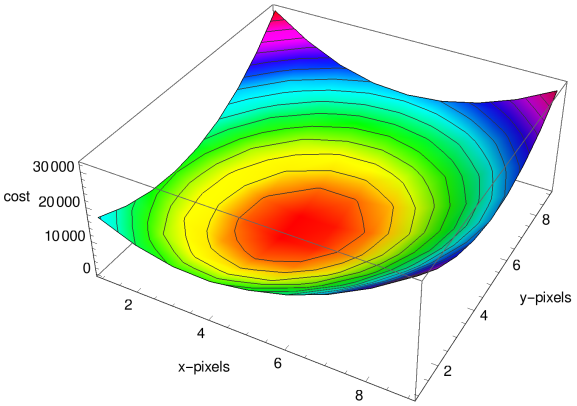

Figure 5: The x, y, and z axis represent the x, y pixels and the cost of the difference between neighboring pixels, respectively. We try to minimize this cost function curve.

In practice, for simplicity, we do not compute the inverse cos and change this angle function to approximately return the number of bit transitions:

$$angle(a,b) = \left(1 - \left(\frac{a \cdot b}{\|a\|\|b\|}\right)\right) * \frac{n}{2} \tag{9}$$

where n is the number of bits in the code. This cost has a minimum of 0 when a and b are aligned (corresponding to an angle 0°), an average of $n/2$ bits when the angle is 90°, when vectors are uncorrelated, and a maximum of n when the vectors are inversely correlated at 180°.

The optimization estimates the subpixel match by minimizing the cost over possible δ_x and δ_y, starting at discrete position $(\hat{x}, \hat{y})$.

Fig. 4 illustrates the difference between a binary cost function and a continuous cost function. Binary cost function curves feature steps where the gradient is 0. In the continuous cost function, the curves are much smoother and precise, so they are better to be optimized on and the gradient descent can easily find the minimum.

4.4 Gradient Descent

As explained above, we used a gradient descent to reduce the computation time for the subpixel search and increase its accuracy. Gradient descent iteratively converges to the local minimum of a function following the negative direction of the gradient at a current point. We minimize the cost for the angle between the two vectors, explained above in Sec. 4.3. The obtained curve is a bowl-shaped curve. Our cost function lends itself well to the minimization due to its shape, as shown in Fig. 5, as it is locally convex, as required by the gradient descent algorithm.

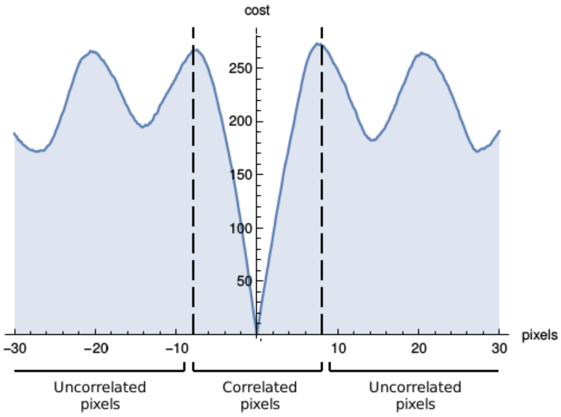

Figure 6: Cost function curve which shows that within a specific neighborhood, ±10 pixels in this case, in the unstructured light pattern, the cost is monotonous and easy to minimize.

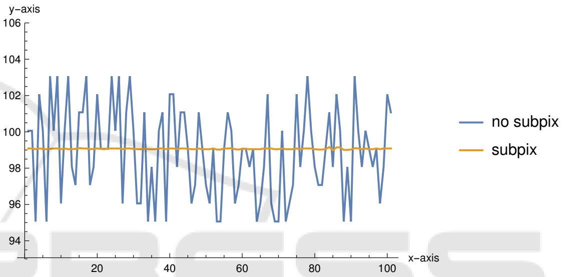

Figure 7: Comparison of matches between matching twice the same reference patterns adding a random noise. The blue curve represents a correspondence without a subpixel accuracy and the orange curve represents a subpixel correspondence. Subpixel accuracy can improve and correct the matching errors in the area where pixels are correlated.

4.5 Correcting Match Errors

An important property of unstructured light patterns is the correlation of the neighboring pixels. On the contrary, there is no correlation between two distant pixels because the patterns are generated randomly. Fig. 6 illustrates the two parts of our cost function and displays at which point is there no more correlation between pixels. Using LSH to establish the pixel correspondences between the camera and the projector generates several matching errors featuring a small deviation from the correct match. The subpixel computation can correct these matching errors, if the corresponding pixel is part of the neighborhood where pixels are correlated. However, if there is no correlation then the subpixel cannot find the correct match. Thus, LSH errors can be compensated by our subpixel method in some cases, namely local matching errors.

For the sake of illustration, the same reference patterns were matched twice adding a noise (±4 randomly to each matched pixel), a first time without subpixel and a second time with the subpixel matching. This noise generates a lot of LSH errors. Fig. 7 illustrates the improvement of the matches.

In addition, if the frequency is very low then the subpixel can improve and correct the matches because the correlated neighborhood is wider. On the other hand, if the frequency is very high, the subpixel has a small area of convergence and can no longer correct large matching errors (see Fig. 2). An example where this matters is if you want to scan faces. In this case, there is an upper limit to the usable frequency since skin presents subsurface scattering which blurs high frequencies. Nevertheless, our subpixel method can compensate for the matching errors and increase the accuracy and the quality of matches.

5 EXPERIMENTS

This section presents various experiments to evaluate our method in real scenes as well as compare it to other methods. Furthermore, the experimental setup used to achieve these experiments is described. Finally, two sets of results are provided; quantitative results to compare subpixel accuracy between our method and other methods, and qualitative results to compare the quality of 3D models generated by different methods.

In all the experiments, common off-the-shelf equipment is used. The camera is a raspberry PI at a resolution of 1280x720 and the projector is an Aaxa HD Pico projector at its native resolution of 1280x720. The projection and the capture are accomplished at 30 fps. Many difficulties were encountered with this common material such as the *auto gain*, the *auto focus* and *flicker*. *Auto gain* is the automatic brightness adjustment of the camera to the illumination of the scene. *Auto focus* is the focus done automatically by the camera to the scene depths. This can thus change the calibration. Finally, flicker is the mixture of colors that the camera sees. To project an RGB image, most RGB projectors send one color at a time, and should the camera have a very short exposure time, then it can distinguishe a mixture of each color. Thus, it is no longer possible to triangulate and obtain 3D models. The camera-projector system was calibrated with a simple planar calibration (Zhang, 2000; Salvi et al., 2002). In addition, our experiments were performed in difficult conditions with a rolling shutter camera.

To evaluate the proposed method, it is compared to the unsynchronized unstructured method without subpixel (El Asmi and Roy, 2018) and to the *Phase Shift* method (Srinivasan et al., 1984). In our experiments, a looping video of 60 unstructured light patterns is projected at 30 fps without synchronization between the projector and the camera. Furthermore, in order to unwrap the phase for the *Phase Shift* method, 16 patterns of a shifted sine (8 patterns for each axis) are added to the 60 unstructured light patterns. The decoding step is performed with the unstructured light patterns then the subpixel is computed from the recovered phases. Because the video is projected and captured at 30 fps, it is important to find the mixture between two consecutive patterns using the unsynchronized unstructured light method.

In this section are presented a first set of results which consist of a quantitative comparison between the three methods, then a second set which consists of a qualitative comparison. The experiments are accomplished on different real scenes; a plane, a specular corner and a Lambertian robot. The results presented above are the raw data obtained, no median filter or equivalents were applied. For the calculation of the phase in each period, a treatment is performed on the neighboring points to unwrap the phase. Then, for the triangulation of the 3D models, a selection of the 3D points is carried out to remove the outliers or the points with an aberrant depth ($z = \pm 200$), and this for the three methods.

The first experiment is to compare unsynchronized unstructured light methods with and without subpixel accuracy. For this experiment, 60 unstructured light patterns are projected on a plane with a pattern frequency of 50 (number of cycles per image). The pixel ratio of this experiment is equal to 2 (each camera pixel sees 4 neighboring projector pixels, thus 2 pixels per axis). Fig. 8 presents a comparison of the two methods. In this figure, from the projector view, the addition of subpixel precision improves the curve by making it smoother as compared to its counterpart, without subpixel, which has a step function shape. On the other hand, from the camera view, the improvement is minimal because of the pixel ratio. One can say that the camera-projector correspondence already has some level of subpixel accuracy.

For the second experiment, 60 unstructured light patterns and 16 patterns of a shifted sine are projected on a specular corner using a frequency of 50. Furthermore, the same pixel ratio (near 2) has been kept. Fig. 9 (top) shows the curves of the three methods from the camera view; unsynchronized unstructured light method without and with the

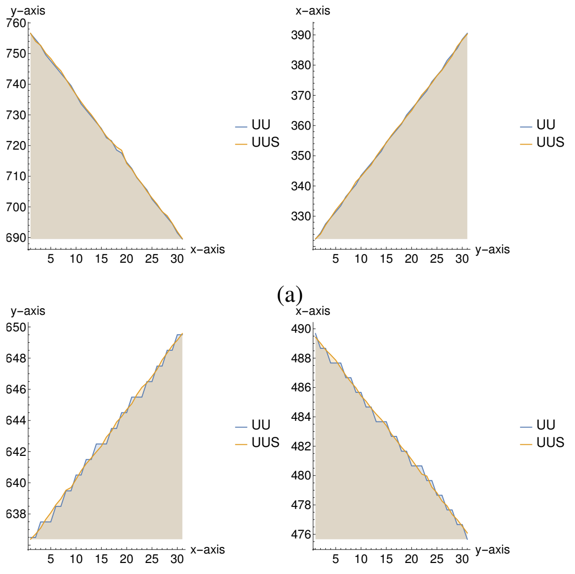

(a)

(b)

Figure 8: The curves represent a line extracted from two LUTs; (a) the camera view and (b) the projector view. The blue curve represents the unsynchronized unstructured light method without the subpixel accuracy (UU) and the orange line represents the unsynchronized unstructured light method with the subpixel accuracy (UUS). The figures left and right represent a number of pixels along the *x* and *y* axis, respectively.

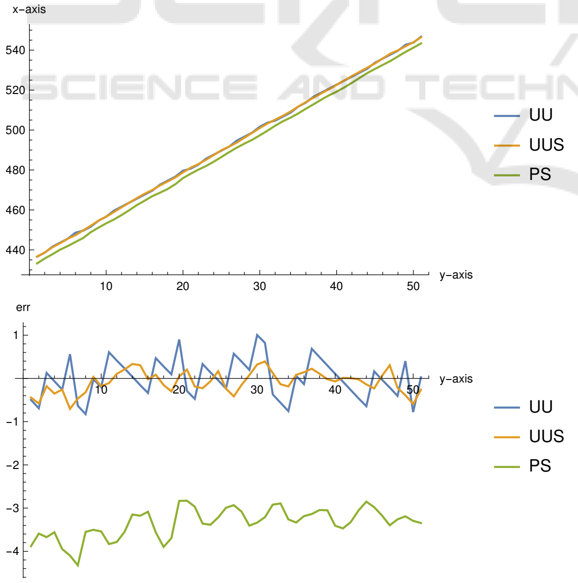

Figure 9: The curves (top) represent a line extracted from three LUTs; the blue curve represents the unsynchronized unstructured light method without the subpixel accuracy (UU), the orange line represents the unsynchronized unstructured light method with the subpixel accuracy (UUS) and the green curve represents the *Phase Shift* method (PS). The curves (bottom) represent the average error between the extracted line and a reference line passing through all the points.

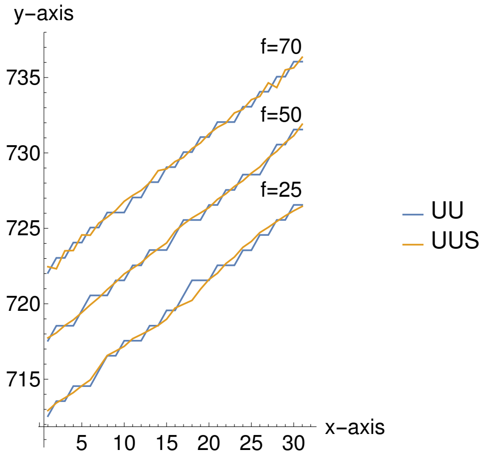

Figure 10: Extracted line from two LUTs of an unstructured light pattern projection with a frequency (f) of 25, 50 and 70; where the frequency represents the number of cycles of each sine per pattern. The blue curve represents the unsynchronized unstructured light method without the subpixel accuracy (UU), the orange line represents the unsynchronized unstructured light method with the subpixel accuracy (UUS).

subpixel accuracy and the *Phase Shift* method. Fig. 9 (bottom) illustrates the average error of each method. The average error is the difference between a line extracted from the LUTs and the reference line. One can notice that there is a slight improvement in the unsynchronized unstructured light method curve with subpixel compared to that without subpixel accuracy. One can further notice that the error curve of the *Phase Shift* method is shifted about 4 pixels because of the specular surface of the reconstructed object.

For the third experiment, the scans are accomplished at different frequencies. As explained in Sec. 3.1, the pattern frequency has a significant impact on subpixel accuracy. Fig. 10 shows a comparison between the unsynchronized unstructured light method with and without subpixel accuracy. The pattern frequency of each scan is {25, 50, 70}. It can be seen that the blue curves with the frequencies 25 and 50 are of step function shape. The curves of the subpixel unsynchronized unstructured light method are much smoother and have no steps. The subpixel corrects even some matching errors because the cost function curve is wider (Fig. 4, freq 25 and 50), so the neighboring pixels are correlated over a larger zone (Fig. 6). On the other hand, the curve with a frequency 70 is less smooth because the cost function curve is very pronounced and the correlation zone is very small (see Fig. 2). The mean and the standard deviation show that the scan at a frequency 70 is better but that the subpixel cannot improve it more as is the case of the frequencies 25 and 50, as

Table 1: The standard deviation of the difference (in pixels) between a reference line and an extracted line from each LUT in x-axis obtained with a different pattern frequency for each set of unstructured light patterns. Mean and std represent the mean and the standard deviation for unsynchronized unstructured light methods with and without subpixel accuracy, respectively.

freq	subpixel	mean	std
25	without	0.255	0.167
	with	0.163	0.112
50	without	0.241	0.169
	with	0.082	0.065
70	without	0.225	0.123
	with	0.140	0.128

Table 2: The standard deviation of the difference (in pixels) between a reference line and an extracted line from each LUT in x-axis obtained with a different pixel ratio for each set of unstructured light patterns. Mean and std represent the mean and the standard deviation for unsynchronized unstructured light methods with and without subpixel accuracy, respectively.

ratio	subpixel	Mean	std
1	without	0.190	0.133
	with	0.088	0.122
2	without	0.148	0.112
	with	0.109	0.084
4	without	0.081	0.059
	with	0.057	0.053

shown in Table 1.

The last experiment in the quantitative results set is the comparison of different pixel ratios. In this experiment, the camera view is chosen and the pattern frequency used is 50. The pixel ratio represents the number of pixels matched between the camera and the projector. We chose three different pixel ratios to demonstrate the achievements of the subpixel accuracy; a camera pixel sees only one projector pixel (ratio = 1), a camera pixel sees 4 projector pixels so 2 pixels per axis (ratio = 2) and finally a camera pixel sees 16 projector pixels so 4 pixels per axis (ratio = 4). Table 2 illustrates the results of the unsynchronized unstructured light method and the subpixel unsynchronized unstructured light method. Mean and standard deviation represent the difference between a line extracted from a LUT and a reference line. The quality of the matches improves when the pixel ratio increases (the average error and the standard deviation decrease). On the other hand, the higher the ratio, the less the subpixel improves the quality as one can say that the correspondence is already subpixel.

For the set of qualitative experiments, four 3D reconstructions obtained with the subpixel unsynchronized unstructured light method and the *Phase Shift* method are presented. Fig. 11 (a) shows a specular corner and Fig. 11 (b) shows a Lambertian robot. The *Phase Shift* model (right (a)) has several holes due to matching errors. These matching errors generate outliers that are removed during the step of calculating polygons to form a 3D model. As a result of the previously mentioned errors, the quality of the matches of the subpixel unsynchronized unstructured light method is deemed superior to the quality of the matches of the *Phase Shift* method. This is because the corner is specular and there is also

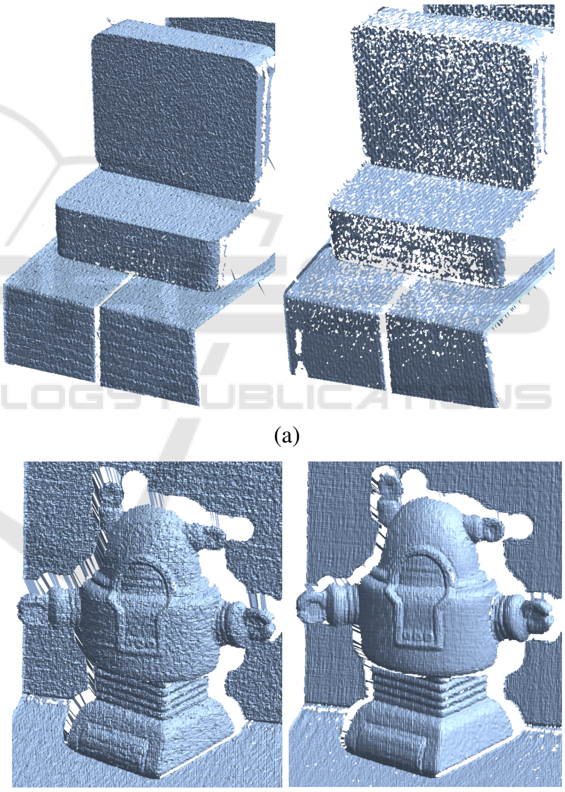
(a)

(b)

Figure 11: Various scenes reconstructed in 3D. (a) shows a 3D reconstruction of a specular corner (a right angle) and (b) shows a 3D reconstruction of a Lambertian robot. The 3D reconstructions (left) are obtained using the unsynchronized unstructured light method with the subpixel precision and the 3D reconstructions (right) are obtained using the *Phase Shift* method. These unfiltered models are obtained from the camera view.

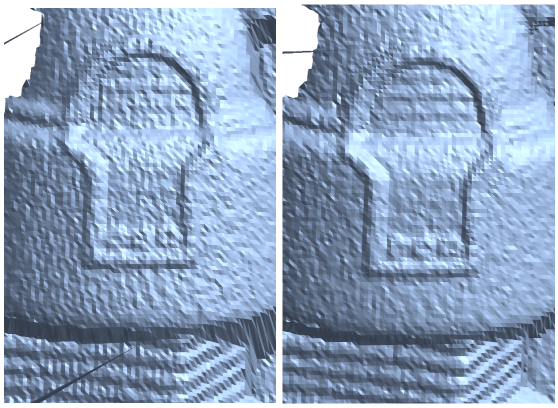

Figure 12: Reconstruction of a Lambertian robot. 3D models are obtained with the unsynchronized unstructured light method without subpixel accuracy (left) and with subpixel accuracy (right). These unfiltered models are obtained from the projector view.

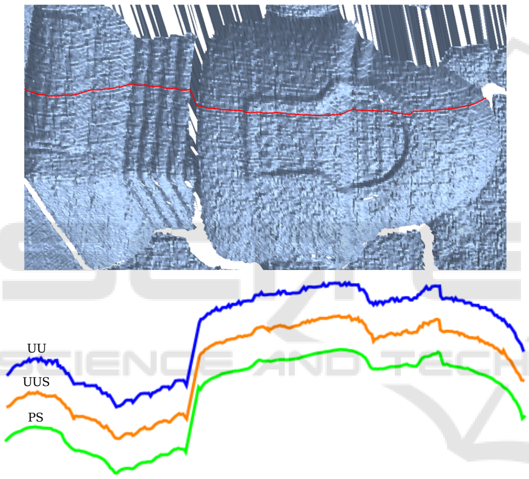

Figure 13: x and y projection (bottom) of reconstructed Lambertian robot for different methods. The blue curve represents the unsynchronized unstructured light method without the subpixel accuracy (UU), the orange line represents the unsynchronized unstructured light method with the subpixel accuracy (UUS) and the green line represents the *Phase Shift* method. The figure (top) illustrates the portion of the robot which is reconstructed.

a mixture between two unstructured light patterns due to the unsynchronized capture. The subpixel unsynchronized unstructured light method is robust to specular objects and to the unsynchronized capture, as shown in Fig. 11 (a) and (b) on the left. Fig. 12 shows a 3D model achieved with the proposed method from the projector view. The cropped image (right) shows more details, obtained through the subpixel precision, than the cropped image (left) which is achieved without subpixel. Fig. 13 illustrates a section of the 3D model (robot). It shows the accuracy of each method on a section of the robot. The quality of the reconstruction is very good and more details can be noticed with subpixel unsynchronized unstructured light and the *Phase Shift* methods.

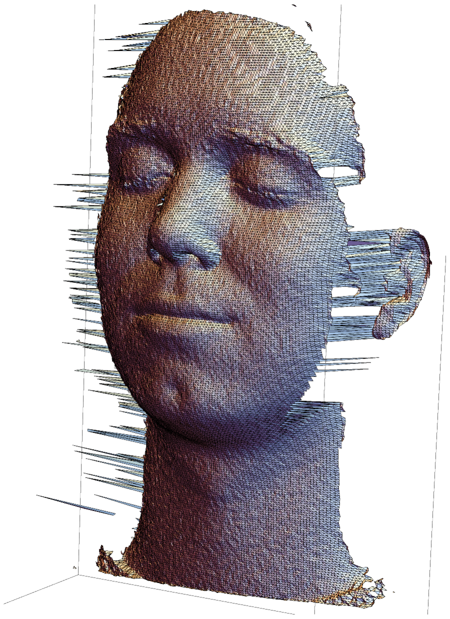

Figure 14: 3D reconstruction using subpixel unsynchronized unstructured light method of a face. This unfiltered model is obtained from the projector view.

The goal of this method is to quickly and efficiently scan faces. In addition to scanning in less than two seconds, the accuracy of the matches is increased by adding subpixel. Fig. 14 illustrates a 3D model of a face from the projector view. An excellent 3D model with the utmost precision is obtained using the proposed method.

6 CONCLUSION

In this article, we proposed a new method to achieve high subpixel accuracy using the unsynchronized unstructured light method. This method increases the precision of the correspondence between the projector and the camera. The unsynchronized unstructured light method makes scanning faces easier in difficult conditions such as subsurface scattering, indirect illumination and scene discontinuities. Relying on low cost hardware without any form of temporal synchronization and a high frame rate, at 30 fps and 60 fps, 3D models with the utmost precision can be achieved. The subpixel estimation is fast and simple, and can also correct errors of the discrete correspondences for a better match quality.

REFERENCES

Andoni, A. and Indyk, P. (2006). Near-optimal hashing algorithms for approximate nearest neighbor in high dimensions. In *Foundations of Computer Science, 2006. FOCS'06. 47th Annual IEEE Symposium on*, pages 459–468. IEEE.

Chen, T., Seidel, H.-P., and Lensch, H. P. (2008). Modulated phase-shifting for 3d scanning. In *Computer Vision and Pattern Recognition, 2008. CVPR 2008. IEEE Conference on*, pages 1–8. IEEE.

Couture, V., Martin, N., and Roy, S. (2011). Unstructured light scanning to overcome interreflections. In *Computer Vision (ICCV), 2011 IEEE International Conference on*, pages 1895–1902. IEEE.

Couture, V., Martin, N., and Roy, S. (2014). Unstructured light scanning robust to indirect illumination and depth discontinuities. *International Journal of Computer Vision*, 108(3):204–221.

El Asmi, C. and Roy, S. (2018). Fast unsynchronized unstructured light. In *Computer and Robot Vision (CRV), 2018 15th Conference on*. IEEE.

Gu, J., Kobayashi, T., Gupta, M., and Nayar, S. K. (2011). Multiplexed illumination for scene recovery in the presence of global illumination. In *Computer Vision (ICCV), 2011 IEEE International Conference on*, pages 691–698. IEEE.

Gühring, J. (2000). Dense 3d surface acquisition by structured light using off-the-shelf components. In *Videometrics and Optical Methods for 3D Shape Measurement*, volume 4309, pages 220–232. International Society for Optics and Photonics.

Gupta, M. and Nayar, S. K. (2012). Micro phase shifting. In *Computer Vision and Pattern Recognition (CVPR), 2012 IEEE Conference on*, pages 813–820. IEEE.

Herakleous, K. and Poullis, C. (2014). 3dunderworld-sls: An open-source structured-light scanning system for rapid geometry acquisition. *arXiv preprint arXiv:1406.6595*.

Huntley, J. M. and Saldner, H. (1993). Temporal phase-unwrapping algorithm for automated interferogram analysis. *Applied Optics*, 32(17):3047–3052.

Inokuchi, S. (1984). Range imaging system for 3-d object recognition. *ICPR, 1984*, pages 806–808.

Jaeggli, T., Koninckx, T. P., and Van Gool, L. (2003). Online 3d acquisition and model integration. In *PROCAMS, ICCV Workshop*.

Koninckx, T. P. and Van Gool, L. (2006). Real-time range acquisition by adaptive structured light. *IEEE transactions on pattern analysis and machine intelligence*, 28(3):432–445.

Kushnir, A. and Kiryati, N. (2007). Shape from unstructured light. In *3DTV Conference, 2007*, pages 1–4. IEEE.

Liu, K., Wang, Y., Lau, D. L., Hao, Q., and Hassebrook, L. G. (2010). Dual-frequency pattern scheme for high-speed 3-d shape measurement. *Optics express*, 18(5):5229–5244.

Martin, N., Couture, V., and Roy, S. (2013). Subpixel scanning invariant to indirect lighting using quadratic code length. In *Proceedings of the IEEE International Conference on Computer Vision*, pages 1441–1448.

Moreno, D., Calakli, F., and Taubin, G. (2015). Unsynchronized structured light. *ACM Transactions on Graphics (TOG)*, 34(6):178.

Nayar, S. K., Krishnan, G., Grossberg, M. D., and Raskar, R. (2006). Fast separation of direct and global components of a scene using high frequency illumination. *ACM Transactions on Graphics (TOG)*, 25(3):935–944.

Rusinkiewicz, S., Hall-Holt, O., and Levoy, M. (2002). Real-time 3d model acquisition. *ACM Transactions on Graphics (TOG)*, 21(3):438–446.

Sagawa, R., Furukawa, R., and Kawasaki, H. (2014). Dense 3d reconstruction from high frame-rate video using a static grid pattern. *IEEE transactions on pattern analysis and machine intelligence*, 36(9):1733–1747.

Salvi, J., Armangué, X., and Batlle, J. (2002). A comparative review of camera calibrating methods with accuracy evaluation. *Pattern recognition*, 35(7):1617–1635.

Salvi, J., Fernandez, S., Pribanic, T., and Llado, X. (2010). A state of the art in structured light patterns for surface profilometry. *Pattern recognition*, 43(8):2666–2680.

Salvi, J., Pagès, J., and Batlle, J. (2004). Pattern codification strategies in structured light systems. *PATTERN RECOGNITION*, 37:827–849.

Srinivasan, V., Liu, H.-C., and Halioua, M. (1984). Automated phase-measuring profilometry of 3-d diffuse objects. *Applied optics*, 23(18):3105–3108.

Takei, J., Kagami, S., and Hashimoto, K. (2007). 3,000-fps 3-d shape measurement using a high-speed camera-projector system. In *Intelligent Robots and Systems, 2007. IROS 2007. IEEE/RSJ International Conference on*, pages 3211–3216. IEEE.

Wang, Y., Liu, K., Hao, Q., Lau, D. L., and Hassebrook, L. G. (2011). Period coded phase shifting strategy for real-time 3-d structured light illumination. *IEEE Transactions on Image Processing*, 20(11):3001–3013.

Wexler, Y., Fitzgibbon, A. W., and Zisserman, A. (2003). Learning epipolar geometry from image sequences. In *Computer Vision and Pattern Recognition, 2003. Proceedings. 2003 IEEE Computer Society Conference on*, volume 2, pages II–209. IEEE.

Wust, C. and Capson, D. W. (1991). Surface profile measurement using color fringe projection. *Machine Vision and Applications*, 4(3):193–203.

Zhang, S., Van Der Weide, D., and Oliver, J. (2010). Superfast phase-shifting method for 3-d shape measurement. *Optics express*, 18(9):9684–9689.

Zhang, S. and Yau, S.-T. (2007). High-speed three-dimensional shape measurement system using a modified two-plus-one phase-shifting algorithm. *Optical Engineering*, 46(11):113603.

Zhang, Z. (2000). A flexible new technique for camera calibration. *IEEE Transactions on pattern analysis and machine intelligence*, 22.